https://doi.org/10.1016/j.jastp.2017.07.008

Fine Spatial Evolution of Leaders and M-components in Rocket-triggered Lightning Observed with a Broadband Interferometer

Mingli Chen[1,*], Yanchi Shen[1], Yaping Du[1], Wansheng Dong[2],

1. The Hong Kong Polytechnic University, Hong Kong SAR, China

* mingli.chen@polyu.edu.hk

2. Chinese Academy of Meteorology Science, Beijing, China

ABSTRACT

Based on measurements of VHF radiation sources and VLF electric fields with a broadband interferometer system, the spatial evolution of leader processes and K-breakdowns and M-components involved in a classically-triggered negative lightning discharge have been analyzed. While a normal classically-triggered negative discharge usually starts with a positive leader initiates from the tip of the ascending triggering-wire and moves upward, there was no such an initial upward positive leader (UPL) being observed for the present discharge, probably due to low resolution and sensitivity of the measurements. Instead, there was a downward negative leader (PDL) at the preliminary stage of the discharge being observed, followed by a 173-ms-long lasting M-component-wise process and two leader/return-stroke processes. The PDL was most likely a leader process along the channel trace possibly built by the undetected UPL, as its speed which ranged from 3.7×10^6 m/s to 0.3×10^6 m/s is similar to that of a dart leader in literature. The long lasting M-component-wise process consisted of a slow negative-going change stage (Ma), followed by a fast negative-going change stage (Mb) and then

a slow positive-going change stage (Mc). Ma was found to be intra-cloud negative breakdowns moving towards overhead position of the PDL trace. Mb would be considered as a common M-component (channel brightening), which starts with a K breakdown in cloud (Mb1) moving horizontally towards overhead position of the previous PDL, followed by an event (Mb2) moving up from ground to cloud along PDL trace. As Mb2 reaching the cloud, more new K breakdowns (Mc) appeared in cloud around extremities of the pre-built channels by Ma and Mb. The leader preceding the first return stroke (L1) started inside the cloud and propagated downward to the triggering-wire trace, but with a different channel to that of PDL. As the leader touched the triggering wire trace, it appeared to propagate upward along the same channel of PDL. The upward portion of L1 might be interpreted as a reflection of L1 at top of the triggering-wire trace towards the PDL trace due to the difference in conductivity and potential between the PDL trace, the triggering wire trace and the L1 channel, which was optically invisible but bright in VHF. The speed of the downward portion of L1 decreased from 2.32 to 0.32 $\times 10^6$ m/s as it descended, while that of the upward portion of L1 increased from 0.85 to 2.7 $\times 10^6$ m/s as it ascended. The leader preceding the second return stroke (L2) behaved similarly to L1 but with higher speeds.

Keyword: rocket-triggered lightning, downward leader, K-breakdown, M-component, return stroke, broadband interferometer.

1. INTRODUCTION

Rocket-triggering lightning technology refers to the launch of a small rocket dragging a thin wire into strong electric fields under a thundercloud. The rapid ascending tip of the rocket-wire would break through the corona shield around it and initiates an upward leader to ultimately trigger a lightning discharge. When the wire is grounded the technique is called classical-triggering, while when the bottom of the wire is floated the technique is called altitude-triggering (Rakov and Uman, 2003) [1]. Rocket-triggered lightning was first successfully attempted over sea in United States in 1960 (Newman et al., 1967) [2] and over land in France in 1973 (Fieux et al., 1975) [3]. Thereafter, rocket-triggered lightning has been accomplished successively in Japan (Horii, 1982) [4], China (Liu et al., 1994) [5] and Brazil (Saba et al., 2000) [6], respectively.

A typical classically-triggered lightning discharge usually starts with an upward positive leader (UPL) initiated from the tip of the ascending wire (e.g. Rakov et al., 1998 [7] and Chen et al., 2013 [8]). The process whereby the UPL continuously propagates to the charged cloud and produces continuous current is called initial stage (IS). During the first few milliseconds of the UPL propagating, the triggering wire is vaporized and the current in the channel base abruptly decreases to zero and then reestablishes (Wang et al., 1999 [9]; Rakov et al., 2003 [10]). When the UPL reaches the charge in the cloud, the initial continuous current (ICC) process begins. The ICC is usually accompanied by pulses, which have characteristics similar to those of M-components occurring after the return strokes (Rakov et al., 2001 [11]). After the IS, the

current in the channel might be near zero and followed by downward negative leader/return stroke processes within the same channel of the UPL. However, not all investigated triggered lightning had M-components or return stroke processes.

The term “M-component” was firstly proposed by Malan and Collens (1937) [12] to present the temporary enhancement in luminosity along an existing grounded lightning channel. It was reported to occur either after the return stroke process in natural lightning (Fisher et al., 1993) [13] or during the IS of rocket-triggered lightning (Rakov et al., 1998) [7]. Properties of the luminosity of M-components, primarily below the cloud bottom, were well-studied by Fisher et al. (1993) [13] and Jordan et al. (1995) [14]. VHF images of M-components, primarily in the cloud in natural lightning, can be found in Shao et al. (1995) [15] and Mazur et al. (1998) [16]. The signature of channel-base currents and the associated electric fields of M-components in triggered lightning was well-addressed by Rakov et al. (2001) [11] and Thottappillil et al. (1995) [17]. A possible mechanism for M-components was proposed by Rakov et al. (1995) [18]: an M-component was a guided-wave process that involves a downward progressing incident wave followed by an upward progressing reflected wave in an existing grounded lightning channel.

In the last two decades, observations with highly-time-resolved optical and electromagnetic field sensors have significantly advanced our knowledge of various lightning leader processes (e.g. Chen et al., 1999 and 2003) [19-20]. In addition, the VHF interferometry technique has been getting more and more popular in the study of lightning inception and development (e.g. Dong et al., 2001and 2003, Kawasaki et al., 2000, Edens et al. 2012) [21-24]. In the following,

the fine spatial evolution of leaders, K-breakdowns and M-components in a classically-triggered lightning discharge observed with a VHF broadband interferometer and a camera will be revisited and discussed.

2. LIGHTING DATA AND LIGHTNING CHANNEL REBUILDING

2.1 Lightning Data

The lightning we analyzed was a rocket-triggered discharge obtained in the summer of 1999 near Guangzhou City in China. The discharge was succeeded at 21:18:36 (Beijing Time) on July 10 of 1999 when the rocket ascended to a height of about 400 m (estimated from the length of the wire the rocket spouted out, which measured about 460 m long and inclined) and the ground electric field was negative just before launch of the rocket.

Shown in Fig. 1 is the observation setup during the experiment, which included a camera, a broadband interferometer (bandwidth 25~100 MHz) and a rocket launcher. The camera and broadband interferometer were located at a distance of 1.3 km west and 90 m south to the rocket launcher, respectively. A slow antenna with a time constant of 6 s (bandwidth 0.03 Hz ~1 MHz) located at the same position of the interferometer was used to record the electric field changes. The broadband interferometer consisted of three identical flat-plane antennas located separately at three apexes of a square with a 10 m baseline on ground. Each of the three antennas was connected via a 50 m coaxial cable to the same 4-channel digital storage oscilloscope (DSO) through a 25 MHz high-pass filters. The record length of each channel is 2 Mega samples. The

DSO sample rate was 1 GHz and its memory of each channel was divided into 2000 segments so as to record the whole process of a discharge. Each segment had a record length of 1000 samples and was pre-triggered by 400 samples. During the data analysis, digital filter was also used to make the VHF data is in the bandwidth of 25~100 MHz. Detailed information of the observation systems was given in (Dong et al., 2001) [21]. For convenience of our analysis, we set the launcher position as the origin of the coordinates, the camera on the X-axis and the interferometer and slow antenna on the Y-axis.

Shown in Fig. 2 is the observed data for the discharge we analyzed. The left panel in the figure is a photograph of the discharge from the camera at 1.3 km west of the discharge, which shows a single channel with typical small horizontal offset between strokes caused by wind. The lower straight part in the photograph is the lightning channel with residual vaporized wire, while the upper bent part, which is estimated to be from about 400 to 900 m above ground, is believed to be the main channel formed by two successive leader-return stroke processes in air. Enlarging the photo, a faintly luminous spot/branch in left of the bright channel around the tip of the triggering wire can be found. The right panel in the figure is the data of the discharge recorded by the interferometer system at 90 m south, which included the electric field changes recorded with the slow antenna (a) and the VHF radiation sources in elevation (b) and azimuth (c). Shown in (d) is the 2D image of VHF sources of the discharge in azimuth and elevation. As the discharge was very close to the sensor, the electric field changes were partly saturated, however, it is still evident that the discharge included a preliminary leader process (P, at time 5 ms),

followed by a long lasting M-component-wise process (M, at time 460 ms) and two successive leader/return stroke processes (R1, at time 608 ms, and R2, at time 786 ms).

2.2 Lightning Channel Rebuilding

The photograph in Fig. 2 is believed to be the image of the bright leader/return stroke channels of the discharge below cloud bottom. It might partly or even not reflect the channels of the preliminary leader process and M-component-wise process of the discharge, but the preliminary leader and M-component-wise process channels would not be so far away from the leader/return stroke channels of the discharge. The VHF radiation sources in Fig. 2 are believed to be associated with breakdown processes involved in all the preliminary leader, the M-component-wise process and the two leader leader/return stroke processes during the discharge. The simplest approach for 3D channel conversion of these processes would be to assume all VHF sources are on a vertical plane going through the trigger launcher site. As shown by the photograph in Fig.2 and later in Figs. 5b and 7b, the leader/return stroke channel inclined to north of the launcher by about 300 m, while the interferometer was only 90 m away from the launcher in south. In such a case, in comparison to the simplest approach, it would be better to rebuild 3D channel images for this discharge by combining the photograph with the VHF radiation source data. The point is that the 3D reconstructed channels for those processes not on the photograph could be affected notably and we should be very careful when explain them. In addition, a positive leader produces less and weaker VHF radiations than a negative leader, which may not be able to trigger a lightning interferometer system. In follows, we first present

the channel rebuilding approach in detail and then an error analysis.

Let the rocket launcher be at the origin in a Cartesian coordinate system (*x, y, z*). The camera is on the x-axis at (x_{cam} = -1300m, 0, 0) and the interferometer is on the y-axis at (0, y_{int} = -90m, 0), as shown by Fig. 1.

For the photograph, each point on the channel image produces a radial line pointing to the real lightning channel in space through the camera, and all such radial lines together would form a curved face in space (*Face 1*). Since a unit length on the photograph represents a certain angle in radian, by referring to a known point on the photograph, the 2D lightning channel on the photograph can easily be converted into a series of elevation and azimuth pair (φ_{1i}, θ_{1i}). Given that the azimuth from the camera to launcher is 0° and it increases counterclockwise, then each pair (φ_{1i}, θ_{1i}) represents a radial line through the camera to the lightning channel in space as,

$$x = z\cot(\varphi_{1i})\cos(\theta_{1i}) + x_{cam}$$

$$y = z\cot(\varphi_{1i})\sin(\theta_{1i}) \quad \ldots\ldots\ldots \quad (1)$$

Where, (i = 1,…, N_1) is a space-resolved direction index of the radial line through the camera to different parts of the lightning channel. All such radial lines together would draw out a curved screen (*Face 1*) that contains the whole lightning channel viewed from the camera. Given that the tip of the triggering wire is 400 m high above ground and 1300 m east from the camera, the raw (φ_{1i}, θ_{1i}) data for the main leader/return stroke channel on the photograph have been obtained and are shown in Fig. 3, which were used to draw *Face 1*.

For the interferometer data, each pair of azimuth and elevation presents a radial line viewed

from the interferometer through the lightning channel in space and hence another curved face (*Face 2*) would be formed. For a lightning process with strong VHF radiations, the interferometer gives a time-resolved series of elevation and azimuth pair (φ_{2j}, θ_{2j}). Given that the azimuth from interferometer to the launcher is 0° and it increases counterclockwise, then each pair (φ_{2j}, θ_{2j}) represents a radial line through the interferometer to the VHF source in space as,

$$x = -z\cot(\varphi_{2j})\sin(\theta_{2j})$$

$$y = z\cot(\varphi_{2j})\cos(\theta_{2j}) + y_{int} \qquad \ldots\ldots\ldots \quad (2)$$

Where, (j = 1,…, N_2) is a time-resolved direction index of the radial line through the interferometer to each VHF source. All such radial lines together draw out a curved face (*Face 2*) that contains all VHF sources sensed by the interferometer during a given time period. Detailed raw (φ_{2j}, θ_{2j}) data from the interferometer for VHF sources during the initial leader process, the two leader/return stroke processes and the M-component are given in Figs. 4, 6, 8 and 10 respectively, which were used to draw *Face 2*.

Theoretically, for the two reader/return strokes that were seen by both the camera and the interferometer, intersection of *Face 2* onto *Face 1* might produce a full 3D channel for them. Projection of *Face 2* onto *Face 1* might also produce a 3D evolution image of the initial leader and M-component channels, but they might not be a true 3D channel since *Face 1* might not contain their full channels. In addition, only the part of the channels within the view of the camera and below the cloud bottom could be reproduced properly. To get the trends of the channels within the cloud, especially for the M-component, the intersection of *Face 2* onto *Face*

1 is capped with a horizontal plane at a fixed height of, say 1500 m, above the ground. The 3D channel rebuilt in such a way might not be a complete 3D one and need to be carefully explained.

In addition, due to the operation principle an interferometer may have big uncertainties for VHF sources close to the interferometer or overhead. Since the present interferometer is only 90 m away from the launcher, an error analysis is needed before channel rebuilding. For a VHF source at (y_j, 0, z_j), its elevation φ_{2j} to the interferometer and the error in the elevation can be estimated by

$$cot(\varphi_{2j}) = \|y_j - y_{int} \pm l/2\|/z_j \qquad \ldots\ldots \quad (3)$$

Where y_{int} = -90 m is the distance of the interferometer to the launcher and l = 10 m is the baseline of the interferometer antenna array. In case $\|y_j - y_{int}\| \gg l/2$ the error will be very small. In case $\|y_j - y_{int}\| \sim l/2$ the error might be significant. For the present case, as shown by the photograph, the triggering wire inclined away from the launcher in the opposite direction to the interferometer. We choose three source positions on the photograph, the highest channel point ($y_1 \approx$ 422m, $z_1 \approx$800m) and the tip ($y_2 \approx$ 276m, $z_2 \approx$400m) and middle ($y_3 \approx$ 138m, $z_3 \approx$200m) points of the triggering wire, for error analysis. By equation (3), the elevation and uncertainty from the interferometer to these three points are φ_{21} =57.38º ± 0.25º, φ_{22} =47.54º ± 0.39º and φ_{23} =41.26º ± 0.63º, respectively. Projection of them onto *Face 1* along *y* direction (θ =180º) by equation (2), the *y* values with their uncertainties for the three sources are estimated as y_1 = 422 ±5 m, y_2 = 276 m ±5 m and y_3 = 138 m ±5 m, respectively. Take account of the interferometer's hardware and

random error of ±0.5º, the uncertainty in *y* dimension when *Face 2* is projected onto *Face 1* should be no more than ±15m for the present case. Similar conclusions could be drawn for the azimuth as well as the *x* and *z* values. For the M-component-wise process, when it is projected on the *z* =1500 m plane and *Face 1*, its uncertainty in *x* or *y* dimension should also be around ±15m. Based on the above analysis, the uncertainty in 3D is estimated as $\pm\sqrt{15^2+15^2+15^2} = \pm 26$, resulting in a space resolution of about 50 m. Therefore, a 3D channel rebuilt in this way should be interpreted based a resolution of about 50 m. These errors will get worse near the ground.

Based on the above proposed method and error analysis, time-resolved 3D channels for the three leader processes and the M-component-wise process of the discharge have been rebuilt and discussed as follows.

3. EVOLUTIONS OF LEADER CHANNELS

3.1 Preliminary Leader Process (P)

Shown in Fig. 4 is an expansion of the electric field changes and VHF sources corresponding to the preliminary leader process (marked P in Fig. 2): a) the electric field change, b) the elevation, c) the azimuth and d) the 2D image in elevation-azimuth. The electric field shows firstly a slow positive-going change during the time of 0 ~ 2ms and then an abrupt change to saturated level at the time of about 2 ms until the time of about 200 ms (also see Fig. 2). Meanwhile, there are only 3 isolated VHF sources detected by the interferometer at the time of 0.877 ms, 1.586 ms and 1.668 ms, respectively, before the abrupt electric field change. The first

two VHF sources have very high elevation values which might be within the cloud, while the third one has a very low elevation which might be around the triggering wire. If there were an upward positive leader initiated from the tip of the triggering wire, it most likely occurred during this time period or even some time before the abrupt electric field, which might be only a faintly luminous channel and was simply missed by both the camera and the interferometer. There are also a few VHF sources with very high elevations and scattered azimuths during the time of about 2 ~ 4 ms after the abrupt electric field change, indicating an intra-cloud activity. Starting from about 4 ms to about 8 ms, there is a series of VHF source locations (see the VHF sources between the two vertical dash lines in Fig. 4 in (b), (c) and (d,)) that show an obvious downward-going trend in elevation, which might be a downward leader along the preceding UPL channel. A decreasing trend in elevation may also be caused by a leader going away from the interferometer, but the decreasing trend in such a case is usually not so steep. To examine this inference, 3D channels for this downward leader (named preliminary downward leader: PDL) were rebuilt and discussed as follows.

Shown in Fig. 5 are the rebuilt 3D channel viewed from the interferometer on x-z plane (a) and from the camera on y-z plane (b) and the channel evolution speed (c) for the PDL of the discharge. Only the part of the channel out of the cloud is shown. It should be noted that such a rebuilt 3D channel is just simply a projection of what seen of the PDL by the interferometer onto the photograph-based *Face 1*. The lightning channel shown by the photograph is believed to be the return stroke channel rather than the PDL channel. The actual PDL channels could be tilted

away from *Face 1*, most likely towards south and overhead of the interferometer, as will be discussed in Sections 3.2 and 4.2. Therefore, the nature of the rebuilt 3D channel in Fig. 5 is still a 2D one, but for easy analysis and comparison against the main leader/return stroke channels. As seen from Fig. 5, the PDL firstly moved from about 930 m high downward to about 300 m high in a vertical manner and then turned to move in a zigzag manner around the triggering wire trace. A question here is why there is no a return stroke immediately following the attachment process being recorded, which normally occurs. A possible reason is that the return stroke following the PDL occurred indeed but was missed by the camera due to bad timing of the photo. And due to the saturation of the electric field at the moment, the return stroke following the PDL can't be confirmed from the electric field record too. The zigzag channel segment might be partially attributed to irregular and diversified breakdown spots around the triggering wire trace. The speed of the PDL varied from 3.7 to 0.3 $\times 10^6$ m/s when it descended from 930 m to 300 m high (shown by black solid-line in Fig. 5) and moved in zigzag towards the triggering wire (shown by red dash-dot-line in Fig. 5). The lower speed in downward stage corresponded to the bending channel part around 500 m to 600 m high. The leader speed showed a general trend of decease as it descended with the time. Since there was no VHF sources observed along the triggering wire trace, we had no mean to determine the speed of the PDL propagating along the triggering wire trace.

3.2 Leader Preceding First Return Stroke (L1)

Shown in Fig. 6 is an expansion of the electric field changes and VHF radiation source data

for the out-cloud part of the first leader/return stroke process (R1) of the discharge in Fig. 2: a) the electric field, b) the elevation, c) the azimuth and d) the 2D image in elevation-azimuth. As seen from the figure, during the time period from 603.8 to 607.3 ms, the leader (L1) was characterized by a slow descending negative electric field change accompanied with many VHF sources located. In contrast to this, the leader after this time period but before the return stroke showed a fast descending negative electric field change with few VHF sources located. This is probably because that the leader just before the return stroke ran downward along the conductive triggering wire trace, resulting in less and weak VHF radiations. The former, which was with many VHF sources located, can be further divided into three stages, namely L1a, L1b and L1c, respectively, as shown in the figure. The elevations of VHF radiation sources showed a descending trend for L1a, a horizontally expanding trend for L1b and a sharply ascending trend for L1c, while the azimuths showed a slowly ascending trend for L1a and L1b but a descending trend for L1c. As will be revealed later on, these three stages had quite different space propagation features from each other.

Shown in Fig. 7 are the rebuilt 3D channel viewed from the interferometer on x-z plane (a) and from the camera on y-z plane (b), and the channel evolution speed (c) for leader L1. It was found that the L1a was a downward propagation stage with a relatively lower speed, while the L1b was a horizontally moving stage around the triggering wire trace and the L1c was an upward propagating stage along the trace of the preceding PDL channel with a relatively higher speed. The L1c (upward) might be interpreted as a branching and reflection of L1a (downward) current

around the triggering wire trace into the trace of the preceding PDL channel, probably due to the big difference in conductivity and potential between L1a, PDL and the triggering wire trace. Such a reflection might be a special phenomenon in this triggered lightning discharge, which was optically invisible to the camera but was well-imaged by the interferometer. Taking account of the continuous negative-going electric field change produced by L1, it is most likely that both L1a and L1c were negatively-charged with L1a going vertically down along *Face 1* and Lc1 going up but tilted away from *Face 1* towards south and overhead position of the interferometer. A negative charge moves from the origin of L1a that is high in cloud and far away from the interferometer into L1c that is close and overhead to the interferometer will produce a continuously negative-going electric field change.

The speed for L1a showed a decrease from 2.32 to 0.32 $\times 10^6$ m/s as it descended, while that for L1c showed an increase from 0.85 to 2.7 $\times 10^6$ m/s as it ascended. The speed for L1b was in a range of 0.4~1.1 $\times 10^6$ m/s. Fig. 7 also means that the wire trace connected to L1 at the end of L1b and the beginning of L1c, where was about 500 m from the ground. The observed time delay between the beginning of L1c and the return stroke was about 1.5 ms, giving a leader velocity of 0.33 $\times 10^6$ m/s along the wire trace. These values are all on the slow side for dart leaders, especially for the path along the conducting triggering wire trace. This is probably due to that the time interval between L1 and previous M-component-wise process is very long (148 ms) and the leader channel analyzed are short and near ground. Jordan et al. (1992) [25] reported an average tendency for dart leader speed to decrease near ground in 12 triggered-lightning strokes in

Florida and 29 leaders in New Mexico triggered lightning. Jordan et al. (1992), for 11 natural lightning strokes and 36 triggered-lightning strokes in Florida and 32 triggered-lightning strokes in New Mexico, also examined dart leader speed as a function of the following return stroke current peak and of the duration of the previous inter-stroke interval. They found, for each of the three data sets analyzed, that dart leader speed and the following return stroke current peak are positively correlated. For all the triggered and natural lightning data taken together there is a weak but statistically significant tendency for lower leader speeds to be associated with longer previous inter-stroke intervals.

3.3 Leader Preceding Second Return Stroke (L2)

Shown in Fig. 8 is an expansion of the electric field changes and VHF radiation source data for the second leader/return stroke process (R2) of the discharge. As shown in the figure, this leader (L2) had a similar feature to that of L1 but with a shorter propagating time period. The L2 can be divided into three stages too, namely L2a, L2b and L2c, respectively. The elevations showed a descending trend for L2a, a horizontally expanding trend for L2b and an ascending trend for L2c, while the azimuths showed an increasing (counter clockwise) trend for L2a and L2b but a decreasing (clockwise) trend for L2c, indicating that they moved in different directions.

Shown in Fig. 9 are the rebuilt 3D channel viewed from the interferometer on x-z plane (a) and from the camera on y-z plane (b) and the channel evolution speed (c) for leader L2. The stage L2a propagated downward in a similar path to L1a but with a higher speed, while the L2b

and L2c are quite similar to L1b and L1c in both the propagation path and speed. Similar to L1c, it is most likely that L2c propagated upward but tilted away from *Face 1* towards south and overhead of the interferometer.

The speed for L2a showed a decrease from 4.13 to 0.5 $\times 10^6$ m/s as it descended, and that for L2c showed an increase from 0.83 to 2.8 $\times 10^6$ m/s as it ascended. The speed for L2b was in a range of 0.5~0.83 $\times 10^6$ m/s. The observed time delay between the beginning of L2c and the return stroke was about 2.8ms, giving a leader velocity of 0.18 $\times 10^6$ m/s along the wire trace. These values are similar to those for L1, which are on the slow side for dart leaders. As discussed in Section 3.2, it is probably because that the time interval between R1 and R2 is very long (178 ms) and the channel analyzed is short and near ground.

4. EVOLUTIONS OF THE M-COMPONENT-WISE PROCESS

Shown in Fig. 10 is an expansion of the electric field and VHF source data for the M-component-wise process of the discharge in Fig. 2, which lasted about 173 ms, much longer than that of M-components reported in literature. As seen from the figure, this long lasting M-component-wise process can be divided into three stages, i.e. stages Ma, Mb and Mc, when the electric field waveforms were referenced. The spatial evolutions for each stage were obtained by projecting the VHF radiation sources onto the photograph-based *Face1* and was capped with the horizontal plane at z =1500 m, as described in Section 2.2. Since the z =1500 m plane and *Face 1* present just the rough positions of the VHF sources of the M-component-wise process inside and below the cloud, respectively, the rebuilt 3D channel might be notably different from

the real one, but it is good for discussion of its possible linkage to the PDL, L1 and L2 processes below the cloud base.

4.1 Stage Ma

The stage Ma corresponded to a slow negative-going electric field change, which lasted about 30 ms and consisted of 5 more small step-wise changes (namely a1, a2, a3, a4 and a5, respectively, in Fig. 10). The 3D channel progression for each small step-wise change of Ma is shown in Figs. 11 & 12, respectively, where the starting point is in red and the ending point is in blue for each small step-wise change.

It is inferred that “a1” is a local breakdown process in cloud at a position far from overhead position of the PDL trace, while “a2” is a breakdown process/streamer extending horizontally from “a1” towards overhead position of the PDL trace at a speed of about 3.2×10^6 m/s (Fig. 11). The “a4” includes 2 source locations: the first one is near the starting location of the “a2” channel and the second one is overhead of the PDL channel. It may be a further development of the “a1” + “a2” channel towards overhead position of the PDL trace. The propagating speed for the “a4” is estimated as 1.9×10^6 m/s (Fig. 12). There were no VHF sources located for “a3” and “a5” which might mean that “a3” and “a5” were just a continuous charge transfer process along “a2” and “a4” channels, respectively. All these suggest that the Ma might be short duration episodes of negative breakdown accompanied with small K-type processes moving towards the flash origin in cloud, the overhead position of the PDL trace.

4.2 Stage Mb

The stage Mb corresponded to a steep and large negative-going electric field change, which lasted about 3 ms and consisted of 2 sub-stages (Mb1 and Mb2) when the VHF radiation sources were examined (Fig. 10). Mb1 started in cloud with 5 VHF sources moving along the trace of Ma (indicated by VHF sources of no.1, 2, 3, 4 and 5 in Fig. 13a) and ended near ground at middle of the wire trace (indicated by the VHF source of no.6 in Fig.13a). With the VHF source of no.6 being considered, Mb1 would be a fast downward-moving process from cloud to ground along firstly the trace of the Ma and then the trace of the PDL (Fig. 13a). The moving speed of Mb1 process was estimated at about 6.2×10^6 m/s, much faster than that of both the Ma and the PDL processes. With the VHF source of no.6 being excluded, Mb would be just a fast K-type breakdown along the Ma trace towards overhead position of the PDL trace. In contrast, Mb2 was found to be a fast upward-moving process started near ground at middle of the wire trace (indicated by the VHF source of no.6 in Fig.14a) and propagated up to cloud along the PDL trace (indicated by VHF sources of no. 7, 8, 9, 10, 11 and 12 in Fig.14a) at a speed of about 2.2×10^6 m/s. It should be noted that the speed here was estimated by capping the channel at a height of 1500 m, while the actual channel could be higher than this (Shao et al., 1995) [15]. This means that the actual speed of Mb2 might be bigger than the speed estimated here. Besides, the long interval between Mb and PDL (about 455 ms long) might lead to a significant decay of the conductivity of PDL trace, hence a lower speed of Mb2 along the PDL trace than that in literature. It is noted that the interferometer got only few VHF sources for the Mb stage and did

not show a connection to the ground. This might be simple due to that the Mb process was along a pre-existing conducting channel built by the PDL so that it emitted weak and few VHF radiations. The steep negative-going electrical field change during Mb might mean that there were large amount of net negative charges being transferred from the far end of Mb1 (the VHF source of no. 1) towards the overhead position of PDL trace or even into the PDL trace. All these suggested that Mb would be an M-component (channel brightening) similar to that in literature, which started with an in-cloud K-type negative breakdown (Mb1) moving horizontally towards the origin of PDL trace, followed by a fast upward positive event (Mb2) moving vertically from ground towards cloud along the PDL trace. Since there were no VHF sources located along the PDL trace for Mb1 and also no optical and current measurements, it was hard to confirm whether Mb1 moved down to the ground.

Based on VHF observations of natural cloud-to-ground lightning, Shao et al. (1995) [15] identified two types M events: i) those initiated by a negative breakdown attaching to a conducting channel to ground during a continuing current stage and ii) those initiated immediately following a return stroke by a positive breakdown and a fast negative recoil event, both were primarily a downward propagating phenomena. It is most likely that Mb might be a type i) M-event but was primarily an upward propagating phenomena.

4.3 Stage Mc

The stage Mc corresponded to a slow positive-going electric field change, which lasted about 140 ms and consisted of 15 more small electric field changes, namely “c1”, “c2”,…, “c15”,

respectively, as shown in Fig. 10. Among them, the “c2”, “c4”, “c6”, “c8”, “c10”, “c11”, “c13” and “c15”, which are characterized by short step-wise negative-going electric field changes, are likely produced by small k-changes in the lightning channel as it extends, as substantiated by Fig.15. The propagation speeds for “c6”, “c8”, “c10” and “c11” were estimated to 7.2×10^4 m/s, 3.2×10^6 m/s, 2.1×10^7 m/s and 4.6×10^6 m/s, respectively. The “c1”, ”c3” ,”c5”,”c7”,”c9”,”c12” and “c14”, which are characterized by smooth positive-going electric field changes and no corresponding VHF sources were located, are inferred to be some continuous current processes transferring negative charges from those channels developed by the Mb, “c2”, “c4”, “c6”, “c8”, “c11” and “c13”, respectively, into the ground. An overview of the Ma, Mb and Mc processes in comparison with the triggering wire and preliminary downward leader channel in 3D is shown in Fig. 16.

5. DISCUSSIONS AND CONCLUSIONS

Based on the data of photograph, the electric field change and VHF radiation sources, a preliminary downward leader (PDL), a long lasting M-component-wise process and two leader/return stroke processes involved in a classically triggered discharge were analyzed. Particularly, we practiced a new technique for 3D channel reconstruction by projecting the time-resolved VHF sources onto a curved screen that is formed from a still photograph for the same lightning discharge. A photograph usually shows the main channel of a leader/return stroke process below the cloud base, while the interferometric VHF sources are mainly emitted from

breakdowns and leader/streamer processes out and in the cloud. Therefore, the rebuilt 3D channels with the present technique for the two leader/return strokes were more or less the true ones, but those for the PDL and the long lasting M-component-wise process might be with notable errors. This means that we need to be very careful when use these rebuilt 3D channel for interpretation of the PDL and the long lasting K-breakdown and M-component-wise process. Nevertheless, the rebuilt 3D channels were much helpful than the raw 2D ones for us to analyze possible correlations between the PDL, the K-breakdown and M-component-wise process and the two leader/return strokes of the present discharge. Major results from these rebuilt 3D channels are summarized and discussed as follows:

a) While a normal triggered discharge usually starts with an initial leader moving from the tip of the ascending rocket upward, there was no such an upward positive leader (UPL) being observed at the preliminary stage of the present discharge, probably due to low resolution and sensitivity of the measurements. In fact, there are also several other studies of triggered lightning with broadband interferometer in China, but all have no obvious UPL being observed. However, there was a downward negative leader at the preliminary stage (PDL) being observed, which moved from the cloud down and attached to the triggering wire trace but with no return stroke immediately following. The speed of the PDL ranged from 3.7 to 0.3×10^6 m/s, which was higher than that of stepped leader but similar to that of dart-stepped leader in literature [1]. A reasonable explanation is that the PDL was a downward moving leader process along the channel trace possibly built by the previous initial UPL.

b) The leader preceding the first return stroke (L1) included three stages: L1a, L1b and L1c. In stage L1a, the leader started inside the cloud and propagated downward, but with a different channel to that of the PDL. In stage L1b, as the leader descended to about 300 m high, it turned to propagate along the same zigzag portion of the previous PDL trace towards the triggering wire trace. In stage L1c, as the leader attached to the triggering wire trace, it turned to propagate upward along the same vertical portion of the previous PDL trace. The speed for L1a showed a decrease from 2.32 to 0.32 $\times 10^6$ m/s as it descended, while that for L1c showed an increase from 0.85 to 2.7 $\times 10^6$ m/s as it ascended. The speed for L1b was in a range of 0.4~1.1 $\times 10^6$ m/s. The speed of L1 along the wire trace was estimated at 0.33 $\times 10^6$ m/s. All these speed values were on the slow side for dart leaders, especially for a conducting wire trace. This might be because that the interval between L1 and previous PDL and M-component was too long (148ms) and the channel analyzed was short and near ground (<900m), as discussed in Section 3.2. The L1c (upward) can be interpreted as a reflection behavior of L1a (downward) around the tip of the triggering wire trace into the previous PDL and M-component channel trace, which was optically invisible but bright in VHF. A possible reason might be that the PDL trace had a lower conductivity than the triggering wire trace and both were with more or less the ground potential (grounded), while the L1a channel was with cloud potential. As a result, the L1 moved partially along the PDL trace upward with relatively strong VHF radiations and partially along the wire trace downward with relatively weak VHF radiations as it attached to the wire trace. Such a phenomenon may also exist in

other upward triggered discharges but is not reported due to lacking of simultaneous optical and VHF observations of this kind of discharges.

c) The leader preceding the second return stroke (L2) behaved similarly to that of L1 but with a higher speed than that of L1. The speed ranges were 0.5~4.13 $\times 10^6$ m/s, 0.5~0.83 $\times 10^6$ m/s and 0.83~2.8 $\times 10^6$ m/s for the L2a, L2b and L2c, respectively. The speed of L2 along the wire trace was estimated at 0.18 $\times 10^6$ m/s. Similar to L1, these low leader speed values might be due to the long time interval (178 ms) between R1 and R2 and the short near ground channel analyzed.

d) The long lasting M-component-wise process following the PDL consisted of a slow negative-going change stage (Ma), followed by a fast negative-going change stage (Mb) and then a slow positive-going recovery change stage (Mc). Stage Ma was found to be intra-cloud episodes of negative breakdown and K- changes moving towards the overhead position of the PDL trace. Stage Mb could be considered as a M-component (channel brightening) similar to that in literature, which started with an in-cloud K breakdown (Mb1) moving horizontally towards the origin of the PDL trace, followed by a positive event (Mb2) moving vertically from ground towards cloud along the PDL trace. As the upward-moving event (Mb2) reached the cloud, more new breakdowns and K streamers (stage Mc) appeared around the in-cloud extremities of pre-built conducting channels by Ma and Mb. The speeds of streamers in stage Ma ranged in 1.9~3.2 $\times 10^6$ m/s and that in stage Mc ranged in 7.2×10^4 m/s ~ 2.1 $\times 10^7$ m/s, which were similar to that of in-cloud streamers in natural lightning by Shao et al. (1995)

[15]. The estimated speed for Mb1 and Mb2 was 6.2 $\times 10^6$ m/s and 2.1×10^6 m/s respectively, which might be too slow for a process moving in the conducting PDL trace. A possible reason might be that we capped the Mb channel at 1500m high for easy analysis, leading to an underestimation of Mb speed. Besides, the long interval between Mb and PDL (about 455 ms) could lead to a significant decay of the conductivity of the PDL trace, hence a lower current propagating speed along it than that in literature.

e) It should be noted that Sun et al. (2013) [26] have located VHF sources on the wire of a triggered discharge, while we have no more VHF sources located along the triggering wire of the present discharge. This could be partially due to that our interferometer system worked at a sequentially triggered mode with a high triggering threshold and relatively weak VHF radiations might be missed. Besides, a short-baseline interferometer with few antennas has difficulty in locating VHF sources if there more than 1 source emitting or if the source is not point-like. In particular, this tends to happen for a leader propagating along the triggering wire near the time of a return stroke and at close distance.

ACKNOWLEDGMENTS

The work leading to this paper was supported by Research Grant Council of Hong Kong Government (Grant no.: PolyU152011/14E). The authors would like to thank all colleagues who have contributed to the relevant rocket-triggered lightning experiments.

REFERENCES

[1] Rakov, V. A., and M. A. Uman (2003), Lightning: Physics and Effects, Cambridge University Press, Cambridge, U. K., p.123, p.164 and pp.265-307

[2] Newman, M. M., J. R. Stahmann, J. D. Robb, Lewis, E. A., S. G. Martin, and S. V. Zinn (1967), Triggered lightning strokes at very close range, *J. Geophys. Res.*, 72 (18), 4671-4674

[3] Fieux, R. P., C. H. Gary, and P. Hubert (1975), Artificially triggered lightning above land, *Nature*, 257, 212-214

[4] Horii, K. (1982), Experiment of artificial lightning triggered with rocket, Mem. Fac. Eng. Nagoya Univ., 34, 77-112

[5] Liu X., C. Wang, Y. Zhang, Q. Xiao, D. Wang, Z. Zhou, and C. Guo (1994), Experiments of artificially triggering lightning in China, *J. Geophys. Res.*, 99 (D5), 10727-10731

[6] Saba, M. M. F., O. Pinto JR, I. R. C. A., Pinto, F. J. Pissolato, A. Eybert-Berard, A. Lefort, C. Potvin, L. F. Heine, and S. Chauzy (2000), An international center for triggered and natural lightning research in Brazil, *In Proc. 2000 Int. Lightning Detection Conf.*, paper 40, 7pp., GAI, 2705 East Medina Road, Tucson, Arizona

[7] Rakov, A. V., M. A. Uman, K. J. Rambo, M. I. Fernandez, R. J. Fisher, G. H. Schnetzer et al. (1998), New insights into lightning processes gained from triggered-lightning experiments in Florida and Alabama, *J. Geophys. Res.*, vol.103, pp.14117-30

[8] Chen, M., D. Zheng, Y. Du, and Y. Zhang (2013), Evolution of line charge density of steadily-developing upward positive leaders in triggered lightning, *J. Geophys. Res. Atmos.*, vol.118, pp.4670–4678, doi:10.1002/jgrd.50446

[9] Wang, D., V. A. Rakov, M. A. Uman, M. I. Fernandez, K. J. Rambo, G. H. Schnetzer, and R. J. Fisher (1999), Characterization of the initial stage of negative rocket-triggered lightning,

J. Geophys. Res., 104(D4), 4213–4222

[10] Rakov, V. A., D. E. Crawford, V. Kodali, V. P. Idone, M. A. Uman, G. H. Schnetzer, and K. J. Rambo (2003), Cutoff and reestablishment of current in rocket-triggered lightning, *J. Geophys. Res.*, 108(D23), 4747, doi:10.1029/2003JD003694

[11] Rakov, V. A., D. E. Crawford, K. J. Rambo, G. H. Schnetzer, M. A. Uman and R. Thottappillil (2001), M-component mode of charge transfer to ground in lightning discharges, *J. Geophys. Res.*, 106(D19), 22817-22831

[12] Malan, D. J., and H. Collens (1937), Progressive lightning III – the fine structure of return lightning strokes, *Proc. Roy. Soc.*, vol. A162, pp. 175-203

[13] Fisher, R. J., G. H. Schnetzer, R. Thottappillil, V. A. Rakov, M. A. Uman and J. D. Goldberg (1993), Parameters of triggered-lightning flashes in Florida and Alabama, *J. Geophys. Res.*, vol.98, pp22887-902

[14] Jordan, D. M., V. P. Idone, R. E. Orville, V. A. Rakov and M. A. Uman (1995), Luminosity characteristics of lightning M components, *J. Geophys. Res.*, vol.100, pp.25695-700

[15] Shao, X. M., P.R. Krehbiel, R.J. Thomas and W. Rison (1995), Radio interferometric observations of cloud-to-ground lightning phenomena in Florida, *J. Geophys. Res.*, vol.100, pp.2749-73

[16] Mazur, V., X.M. Shao and P.R. Krehbiel (1998), “Spider” lightning in intracloud and positive cloud-to-ground lightning flashes, *J. Geophys. Res.*, vol.103, pp.19811-22

[17] Thottappillil, R., J. D. Goldberg, A. V. Rakov, M. A. Uman, R. J. Fisher and G. H. Schnetzer (1995), Properties of M components from currents measured at triggered lightning channel base, *J. Geophys. Res.*, vol. 100, pp. 25711-20

[18] Rakov, A. V., R. Thottappillil, M. A. Uman and P. P. Barker (1995), Mechanism of the

lightning M component, *J. Geophys. Res.*, vol.100, pp.25701-10

[19] Chen, M. N. Takagi, T. Watanabe, D. Wang, Z-I. Kawasaki and X. Liu (1999), Spatial and temporal properties of optical radiation produced by stepped leaders, *J. Geophys. Res.*, Vol.104 (D22), pp.27573-84

[20] Chen, M., T. Watanabe, N. Takagi, Y. Du, D. Wang and X. Liu (2003), Simultaneous observations of optical and electrical signals in altitude-triggered negative lightning flashes, *J. Geophys., Res.*, Vol.108 (D8), 4240, doi:10.1029/2002JD002676

[21] Dong, W., X. Liu, Y. Yu and Y. Zhang (2001), Broadband interferometer observations of a triggered lightning, *Chinese Science Bulletin*, Vol.46, No.18, pp.1561-1565

[22] Dong, W., X. Liu, M. Chen and Y. Zhang (2003), Broadband interferometer observations of the bi-directional breakdown process in natural lightning, *Chinese Journal of Geophysics,* Vol.46, No.3, pp.449-456.

[23] Kawasaki, Z., R. Mardiana and T. Ushio (2000), Broadband and narrowband RF interferometers for lightning observations, *Geophysical research Letters*, Vol.27, No.19, pp.3189-3192, doi: 10.1029/1999GL011058.

[24] Edens, H. E., K. B. Eack, E. M. Eastvedt, J. J. Trueblood, W. P. Winn, P. R. Krehbiel, G. D. Aulich, S. J. Hunyady, W. C. Murray, W. Rison, S. A. Behnke, R. J. Thomas (2012), VHF lightning mapping observations of a triggered lightning flash, *Geophysical research Letters*, Vol.39, No.19, doi: 10.1029/2012GL053666.

[25] Jordan, D. M., V. P. Idone, V.A. Rakov, M.A. Uman, W.H. Beasley, H. Jurenka (1992),

Observed dart leader speed in natural and triggered lightning, *J. Geophys., Res.*, Vol.97, pp.9951-7.

[26] Sun, Z., X. Qie, M. Liu, D. Cao, D. Wang (2013), Lightning VHF radiation location system based on short-baseline TDOA technique - Validation in rocket-triggered lightning, *Atmospheric Research*, Vol.129–130, pp.58–66, doi: 10.1016/j.atmosres.2012.11.010.

CAPTIONS

Fig. 1: The setup of observations during the triggered-lightning experiment in 1999 in Guangzhou, China. X-axis: west to east, Y-axis: south to north.

Fig. 2: Analyzed raw data of the triggered-lightning discharge analyzed. The left panel is a photograph of the discharge from a camera located 1.3 km west of the rocket launcher. The right panel is the electric field changes (a) and the VHF radiation sources in elevation (b) and azimuth (c) and the elevation-azimuth image (d) of the discharge. The azimuth from the interferometer to the launcher on the Y-axis is set to 0° and it increases counterclockwise. The time 0 refers to the triggering time of the slow antenna and the interferometer system.

Fig. 3: Raw azimuth and elevation for the lightning channel on the photograph in Fig. 2, versus the height (z) at x=0 plane. The azimuth from the camera to the launcher on the X-axis is set to 0° and it increases counterclockwise.

Fig. 4: Expansion of the electric field (a), VHF source elevation (b) and azimuth (c) and the elevation-azimuth image (d) for the preliminary stage (P) in Fig. 2. The data between the two vertical dash lines are used for rebuilding the 3D channel.

Fig. 5: Rebuilt 3D channels viewed from the interferometer on x-z plane (a) and from the camera on y-z plane (b) and the channel evolution speed (c) for the downward leader (PDL) during the preliminary stage (P) of the discharge in Fig. 2. The blue dash-line represents the triggering wire trace. The blue dot-line represents the triggering wire trace. The black and red lines are for the leader channel at downward-moving and

zigzag-moving stages, respectively.

Fig. 6: Expansion of the electric field (a), VHF source elevation (b) and azimuth (c) and the elevation-azimuth image (d) for the first leader/return stroke (L1/R1) in Fig. 2.

Fig. 7: Rebuilt 3D channels viewed from the interferometer on x-z plane (a) and from the camera on y-z plane (b) and the channel evolution speed (c) for the leader (L1) preceding the first return stroke (R1). The blue dot-line represents the triggering wire trace. The black, red and purple lines are for the leader at downward, zigzag and upward stages, respectively.

Fig. 8: Expansion of the electric field (a), VHF source elevation (b) and azimuth (c) and the elevation-azimuth image (d) for the second leader-return stroke (L2/R2) in Fig. 2.

Fig. 9: Rebuilt 3D channels viewed from the interferometer on x-z pane (a) and from the camera on y-z plane (b) and the channel evolution speed (b) for the leader (L2) preceding the second return stroke (R2). The blue dot-line represents the triggering wire trace. The black, red and purple lines are for the leader at downward, zigzag and upward stages, respectively.

Fig. 10: Expansion of the electric field (a), the VHF source elevation (b) and azimuth (c) and the elevation-azimuth image (d) for the M-component-wise process of the discharge in Fig. 2. The M process was divided into three stages, Ma, Mb and Mc, respectively.

Fig. 11: Rebuilt 3D evolution of “a2” of Ma of the M-component-wise process (a), that viewed from the interferometer on x-z plane (b) and that viewed from the camera on y-z plane

(c). Red "+" was for the starting point and blue "+" for the ending point for "a2" process.

Fig. 12: Similar to Fig. 11 but for "a4" of Ma of the M-component-wise process.

Fig. 13: Similar to Fig. 11 but for Mb1 of Mb of the M-component-wise process. The numbers (1, 2, 3, 4, 5 and 6) indicate the VHF sources' time sequence. Mb1 starts (red "+") in cloud and goes down to ground (blue "+") along the PDL channel.

Fig. 14: Similar to Fig. 11 but for Mb2 of Mb of the M-component-wise process. The numbers (6, 7, 8, 9, 10, 11 and 12) indicate the VHF sources' time sequence. Mb2 starts (red "+") near ground and goes up to cloud (blue "+") along the PDL channel.

Fig. 15: Similar to Fig. 11 but for whole Mc stage of the M-component-wise process. The Mc process consists of c1, c2, c3…c15. It seems that they likely are small k-changes produced in the Ma and Mb channel as it extends.

Fig. 16: An overview of the Ma, Mb and Mc processes in comparison with the triggering wire and preliminary downward leader channel in 3D.

FIGURES:

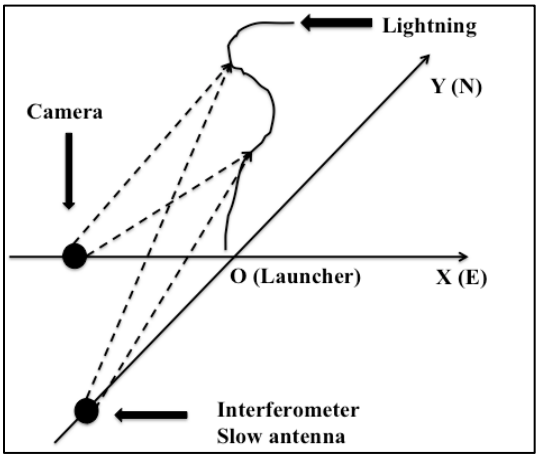

Fig. 1: The setup of observations during the triggered-lightning experiment in 1999 in Guangzhou, China. X-axis: west to east, Y-axis: south to north.

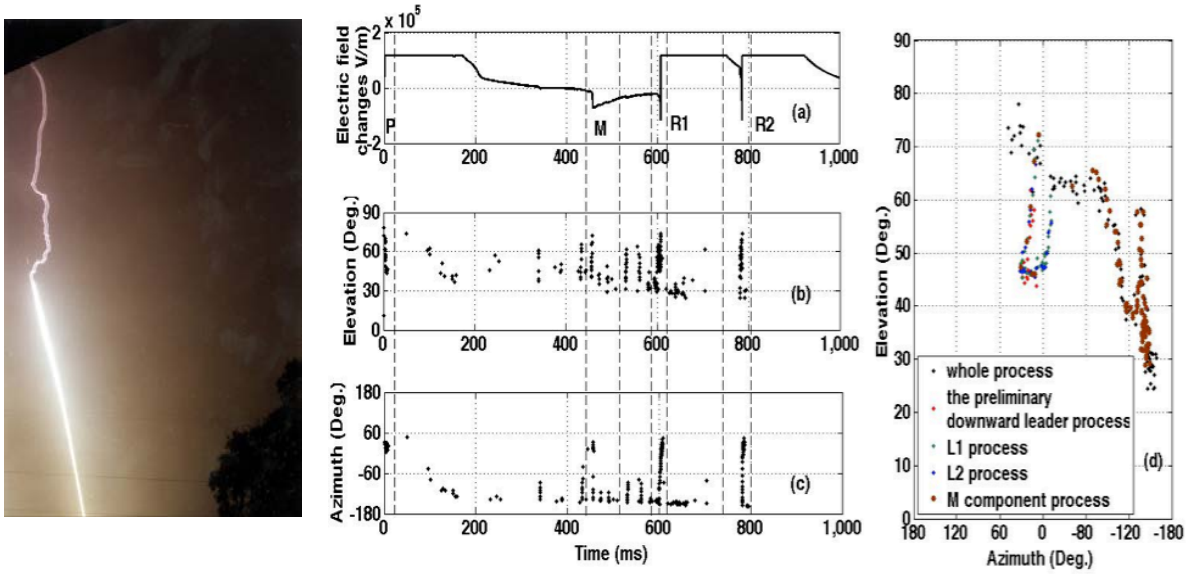

Fig. 2: Analyzed raw data of the triggered-lightning discharge analyzed. The left panel is a photograph of the discharge from a camera located 1.3 km west of the rocket launcher. The right panel is the electric field changes (a) and the VHF radiation sources in elevation (b) and azimuth (c) and the elevation-azimuth image (d) of the discharge. The azimuth from the interferometer to the launcher on the Y-axis is set to 0° and it increases counterclockwise. The time 0 refers to the triggering time of the slow antenna and the interferometer system.

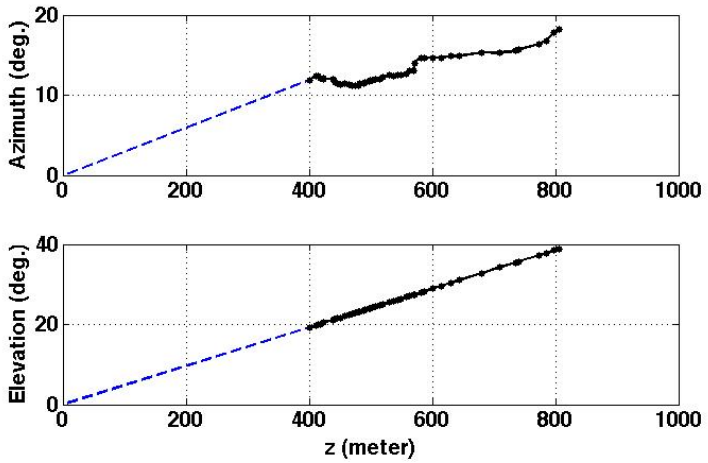

Fig. 3: Raw azimuth and elevation for the lightning channel on the photograph in Fig. 2, versus the height (z) at x=0 plane. The azimuth from the camera to the launcher on the X-axis is set to 0° and it increases counterclockwise.

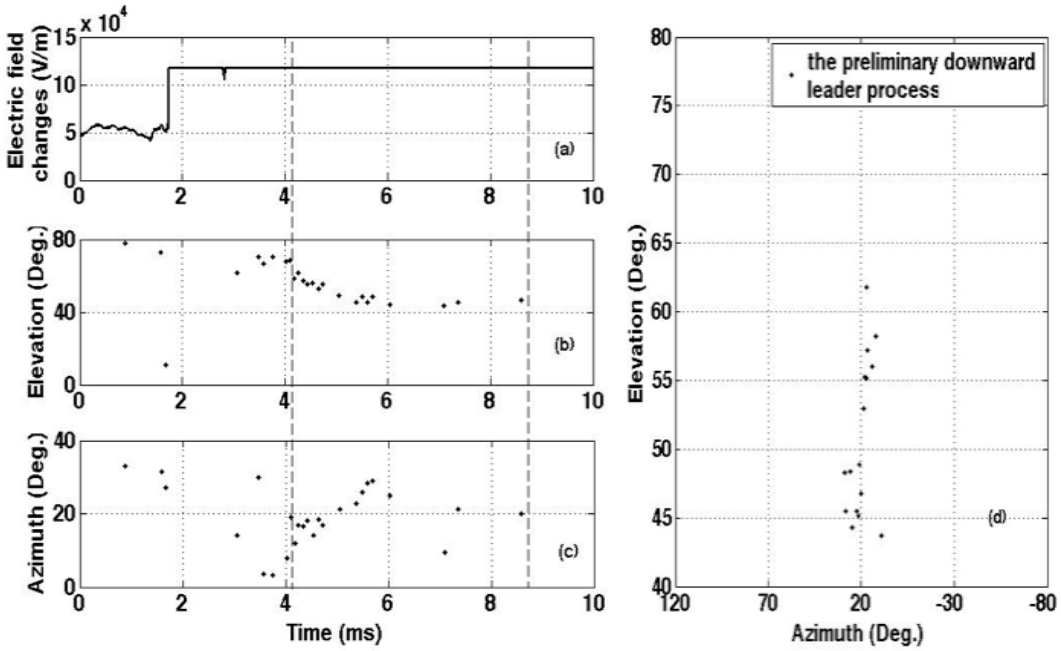

Fig. 4: Expansion of the electric field (a), VHF source elevation (b) and azimuth (c) and the elevation-azimuth image (d) for the preliminary stage (P) in Fig. 2. The data between the two vertical dash lines are used for rebuilding the 3D channel.

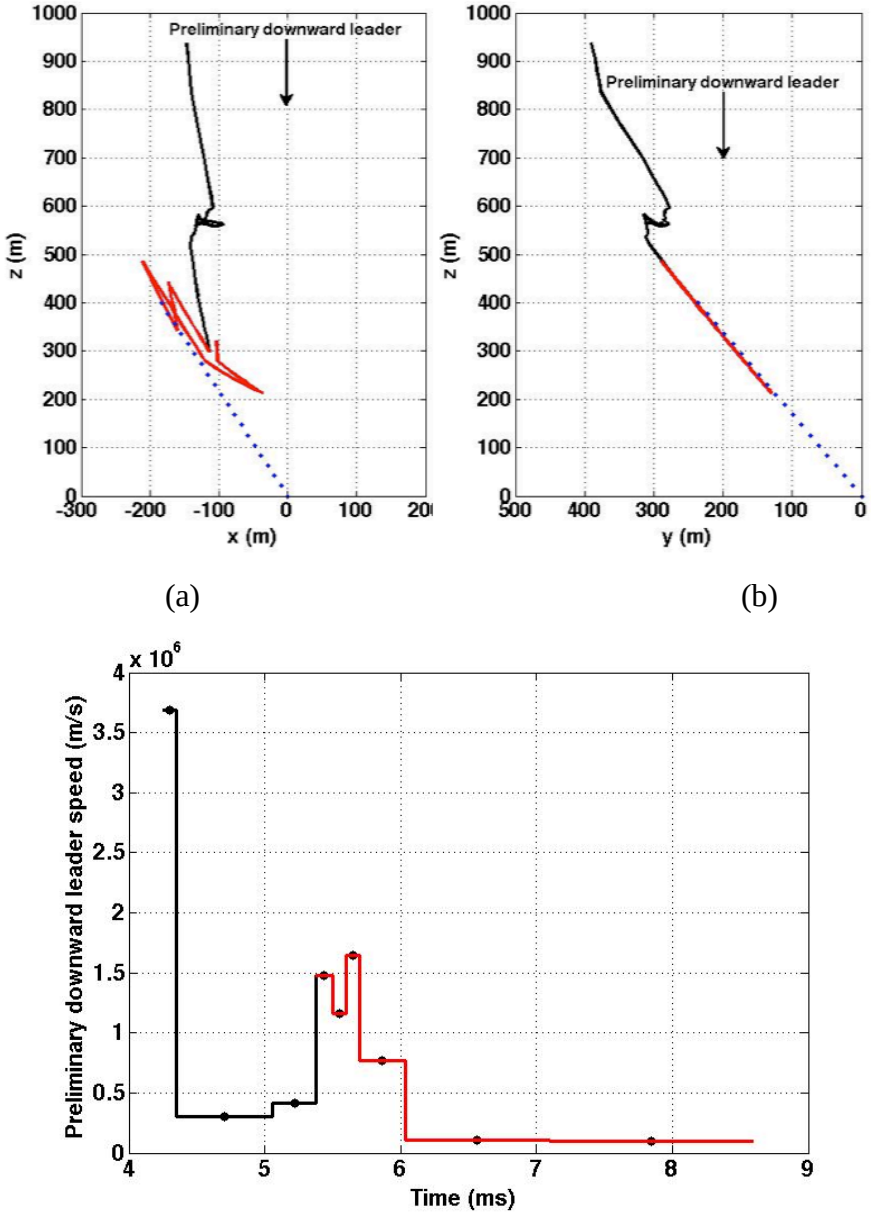

Fig. 5: Rebuilt 3D channels viewed from the interferometer on x-z plane (a) and from the camera on y-z plane (b) and the channel evolution speed (c) for the downward leader (PDL) during the preliminary stage (P) of the discharge in Fig. 2. The blue dot-line represents the triggering wire trace. The black and red lines are for the leader channel at downward and zigzag stages, respectively.

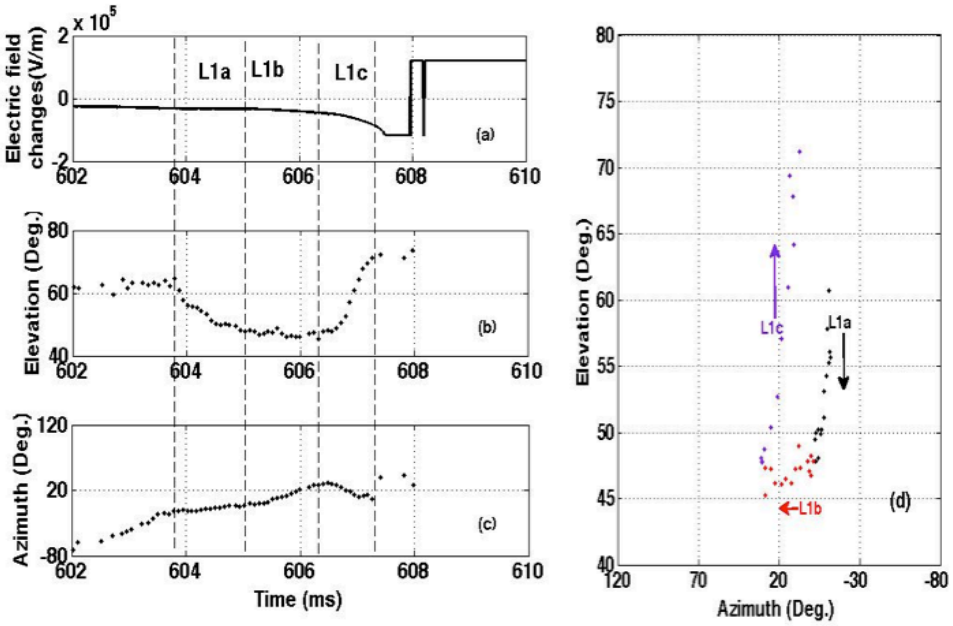

Fig. 6: Expansion of the electric field (a), VHF source elevation (b) and azimuth (c) and the elevation-azimuth image (d) for the first leader/return stroke process (L1/R1) in Fig. 2.

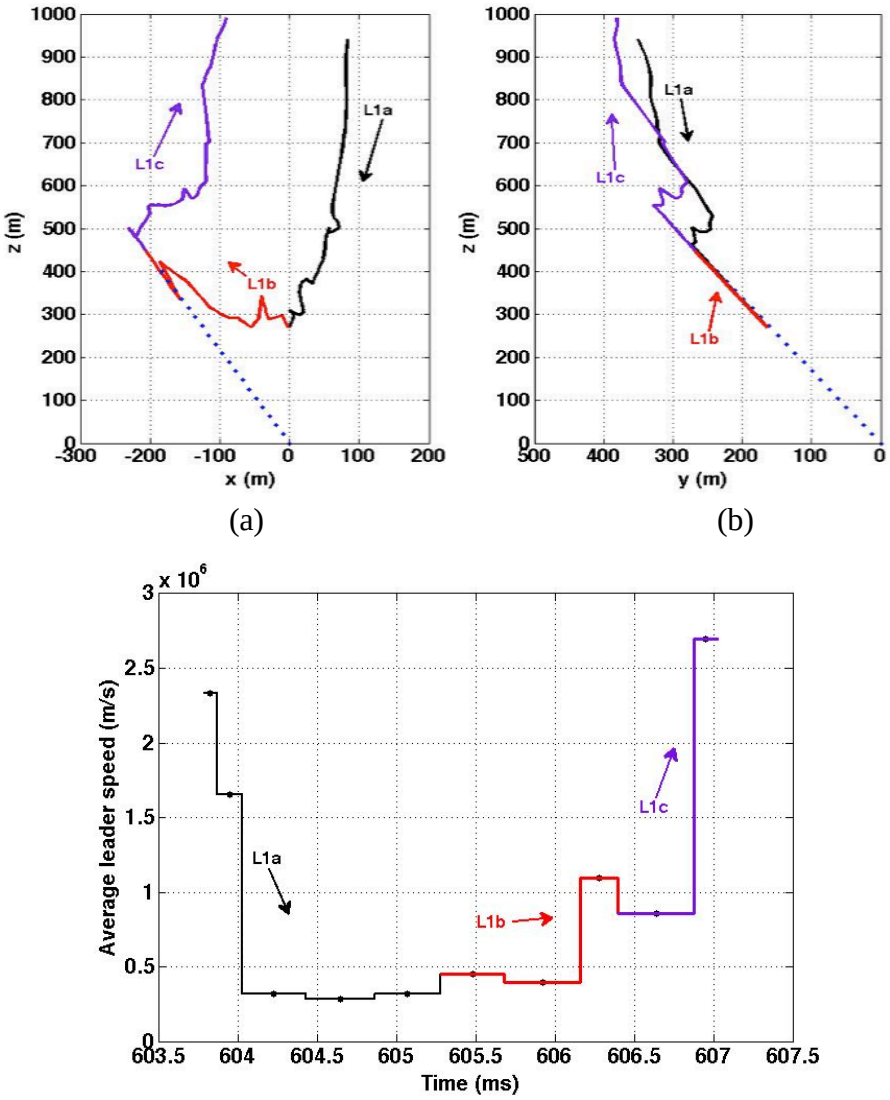

Fig. 7: Rebuilt 3D channels viewed from the interferometer on x-z plane (a) and from the camera on y-z plane (b) and the channel evolution speed (c) for the leader (L1) preceding the first return stroke (R1). The blue dot-line represents the triggering wire trace. The black, red and purple lines are for the leader at downward, zigzag and upward stages, respectively.

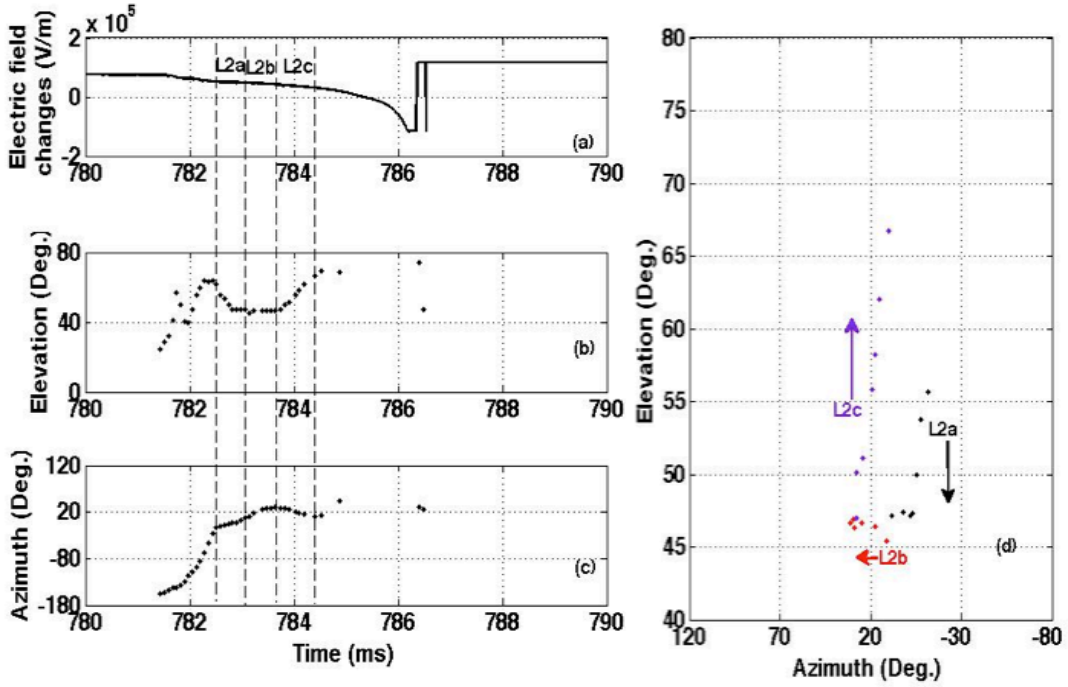

Fig. 8: Expansion of the electric field (a), VHF source elevation (b) and azimuth (c) and the elevation-azimuth image (d) for the second leader-return stroke process (L2/R2) in Fig. 2.

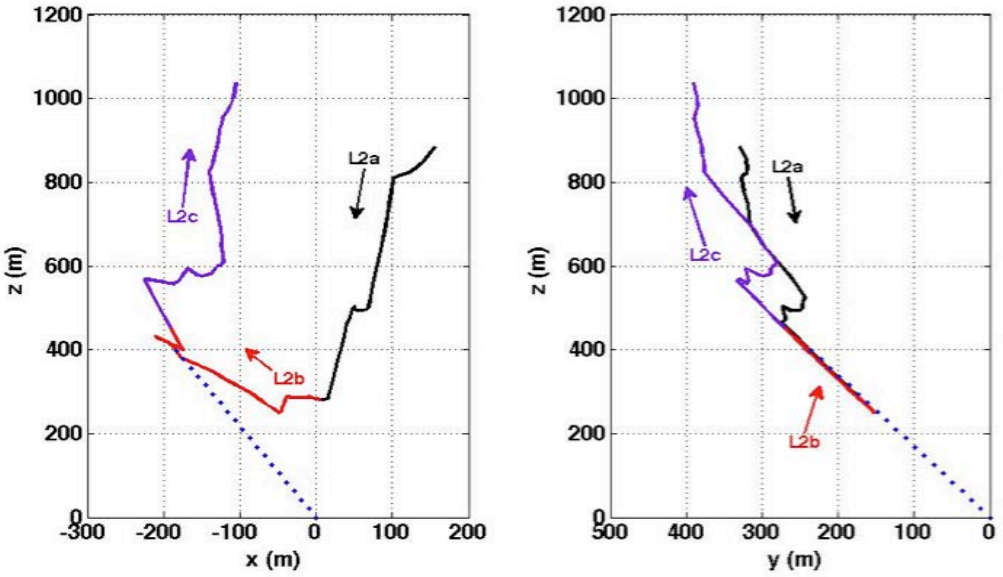

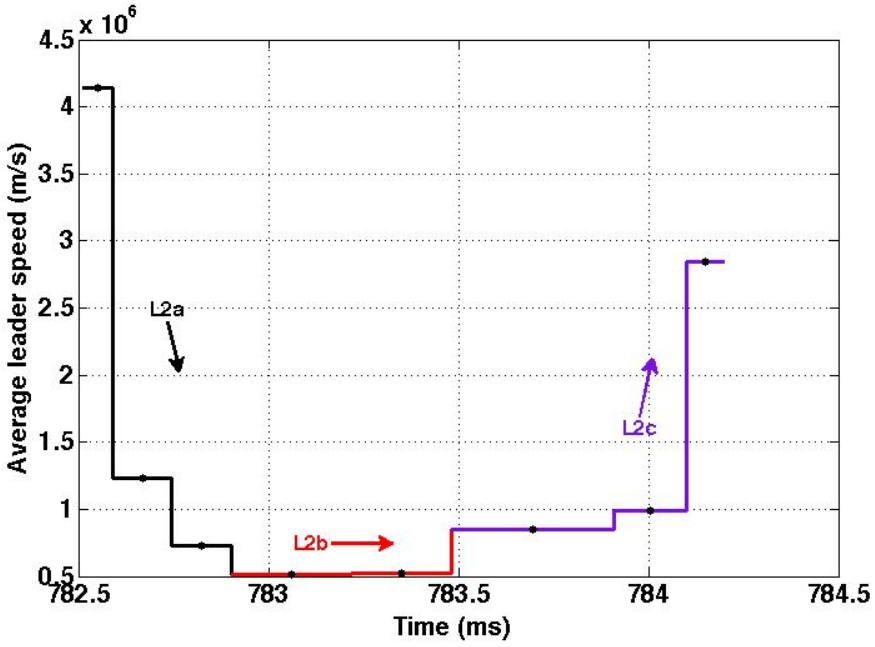

Fig. 9: Rebuilt 3D channels viewed from the interferometer on x-z plane (a) and from the camera on y-z plane (b) and the channel evolution speed (c) for the leader (L2) preceding the second return stroke (R2). The blue dot-line represents the triggering wire trace. The black, red and purple lines are for the leader at downward, zigzag and upward stages, respectively.

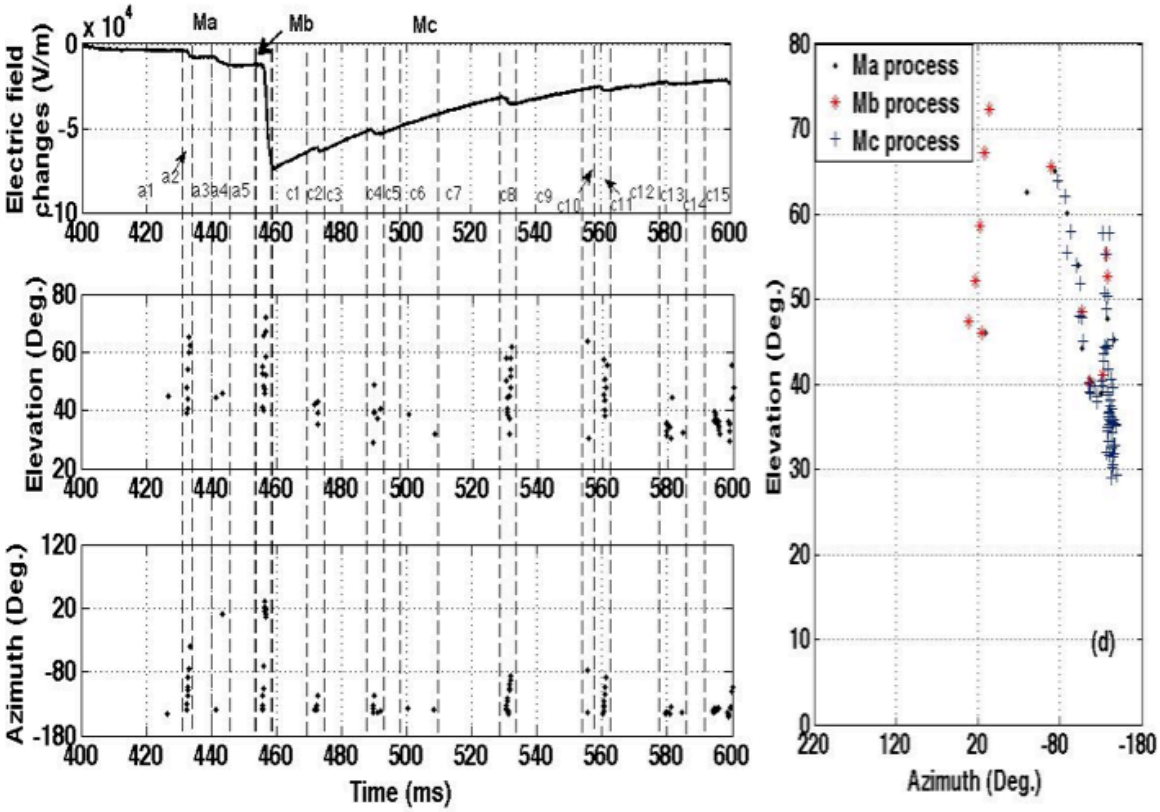

Fig. 10: Expansion of the electric field (a), the VHF source elevation (b) and azimuth (c) and the elevation-azimuth image (d) for the M-component-wise process of the discharge in Fig. 2. The M process was divided into three stages, Ma, Mb and Mc, respectively.

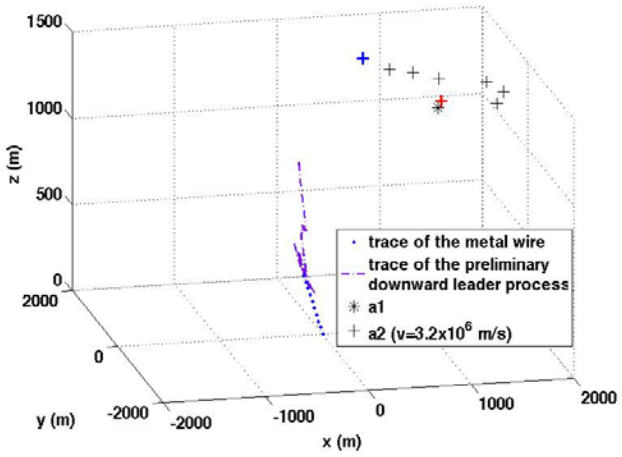

(a)

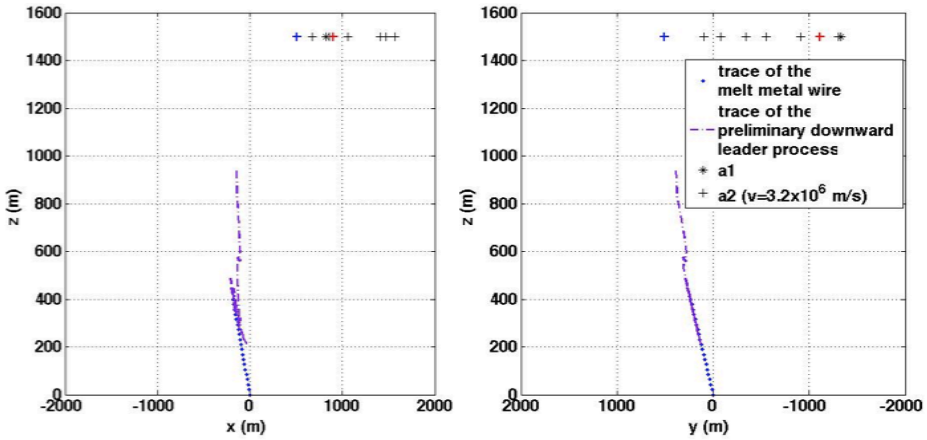

(b) (c)

Fig.11: Rebuilt 3D evolution of "a2" of Ma of the M-component-wise process (a), that viewed from the interferometer on x-z plane (b) and that viewed from the camera on y-z plane (c). Red "+" was for the starting point and blue "+" for the ending point for "a2" process.

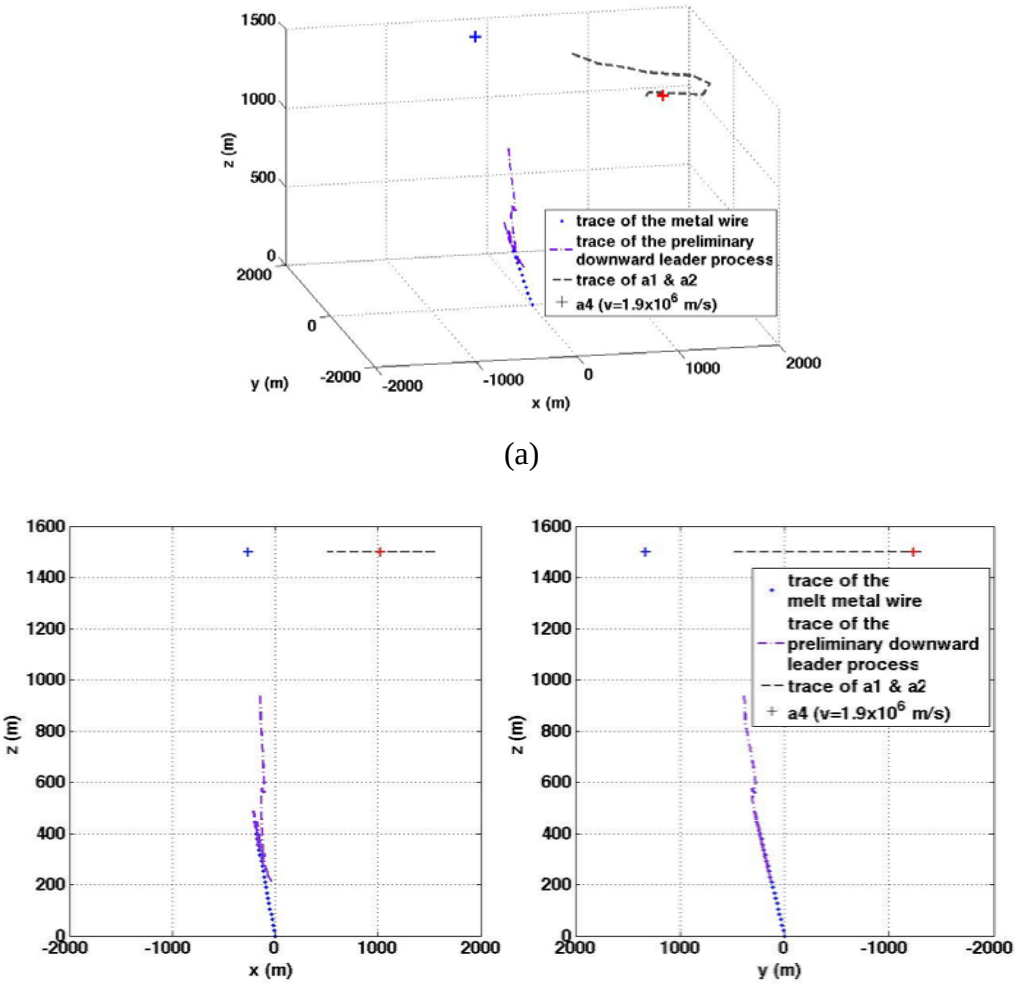

Fig. 12: Similar to Fig. 11 but for "a4" of Ma of the M-component-wise process.

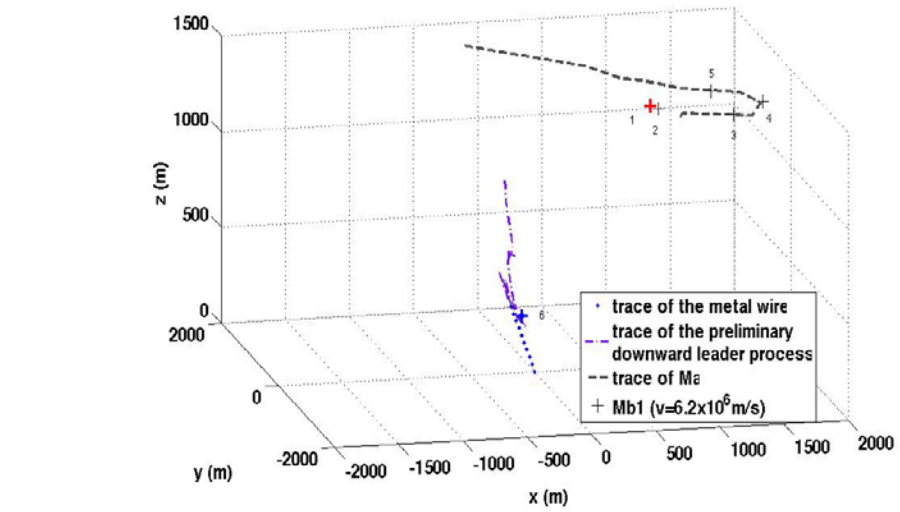

(a)

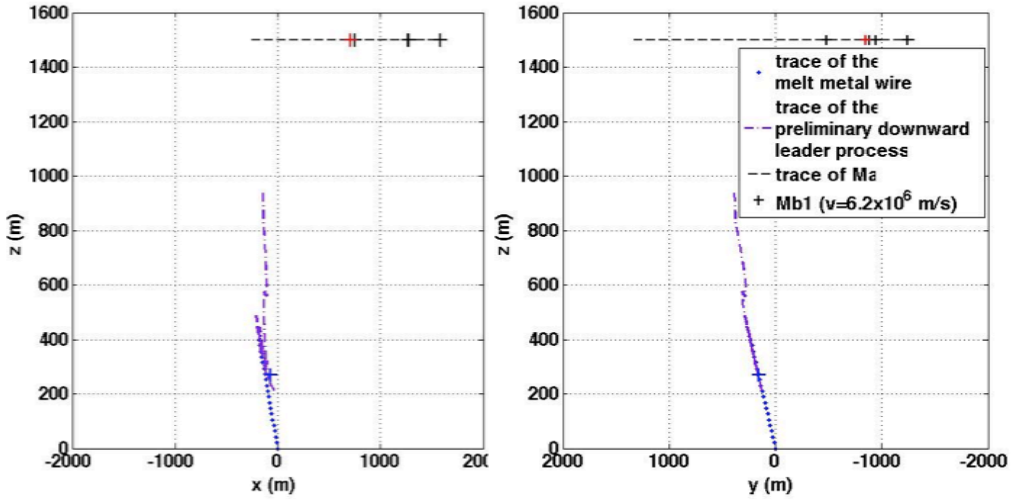

(b) (c)

Fig. 13: Similar to Fig. 11 but for Mb1 of Mb of the M-component-wise process. The numbers (1, 2, 3, 4, 5 and 6) indicate the VHF sources' time sequence. Mb1 starts (red "+") in cloud and goes down to ground (blue "+") along the PDL channel.

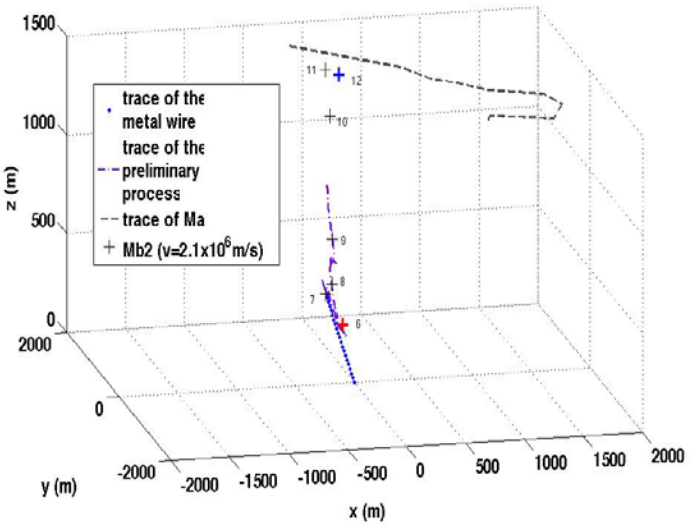

(a)

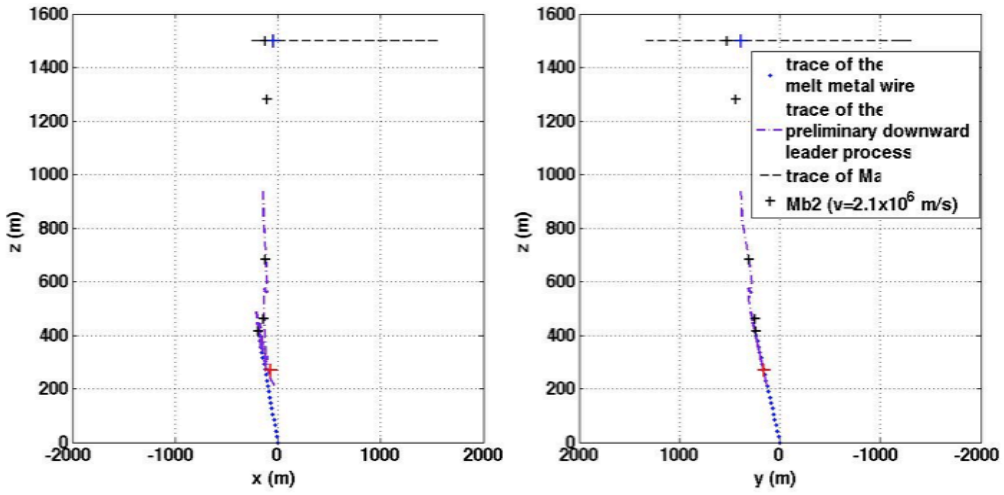

(b) (c)

Fig. 14: Similar to Fig. 11 but for Mb2 of Mb of the M-component-wise process. The numbers (6, 7, 8, 9, 10, 11 and 12) indicate the VHF sources' time sequence. Mb2 starts (red "+") near ground and goes up to cloud (blue "+") along the PDL channel.

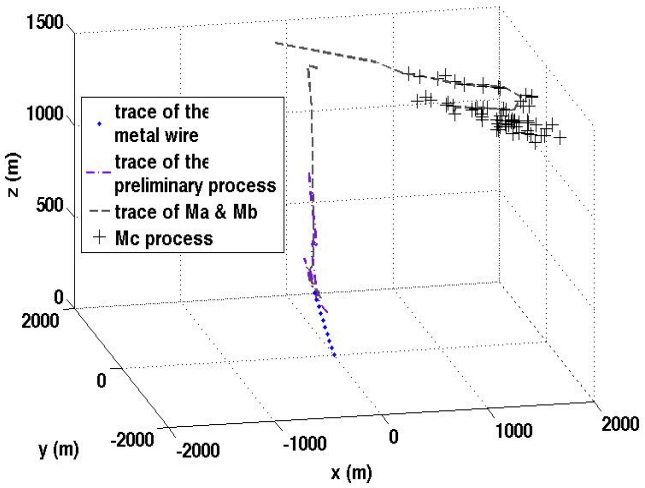

(a)

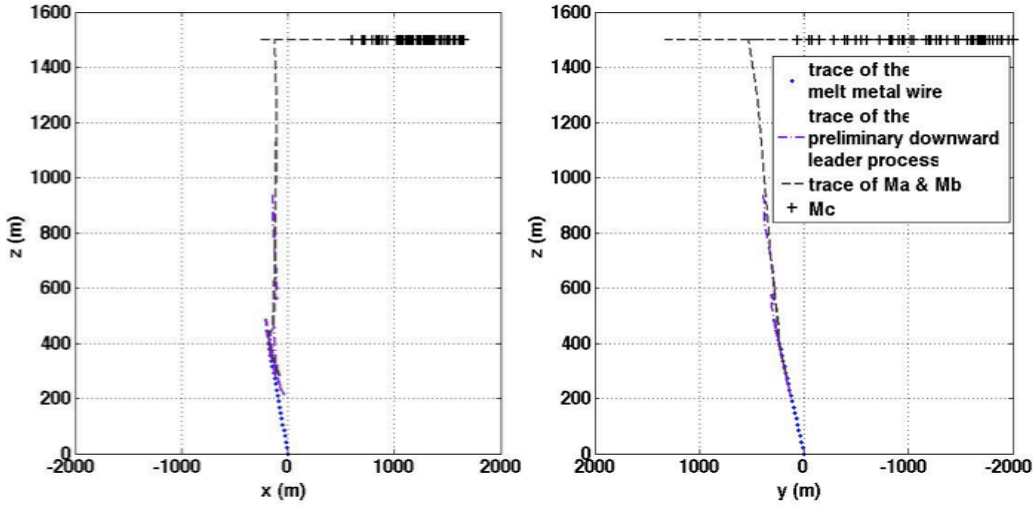

(b) (c)

Fig. 15: Similar to Fig. 11 but for whole Mc stage of the M-component-wise process. The Mc process consists of c1, c2, c3…c15. It seems that they likely are small k-changes produced in the Ma and Mb channel as it extends.

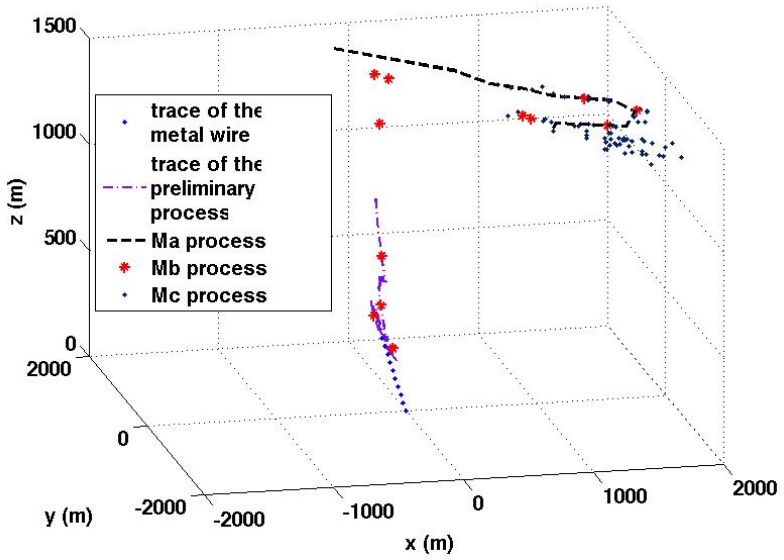

Fig. 16: An overview of the Ma, Mb and Mc processes in comparison with the triggering wire and preliminary downward leader channel in 3D.